A&A 451, 1117–1124 (2006)
DOI: 10.1051/0004-6361:20054391
© ESO 2006

Astronomy & Astrophysics

Hall effects on dynamic magnetic reconnection at an X-type neutral point⋆

T. Senanayake and I. J. D. Craig

Department of Mathematics, University of Waikato, Private Bag 3105, Hamilton, New Zealand
e-mail: sts1@math.waikato.ac.nz

Received 21 October 2005 / Accepted 3 February 2006

ABSTRACT

Aims. The goal of this paper is the examine the impact of the Hall current effects on magnetic reconnection solutions.
Methods. The problem of perturbing a line-tied current free X-point equilibrium is considered. Computational results are presented which highlight how Hall currents influence the initial reconnection rate and the later asymptotic decay.
Results. Resistive scaling laws are derived which quantify the decay rates of perturbations in terms the dimensionless resistivity η of the plasma, and the ion skin depth d_i. Numerical computations confirm that the solution geometry changes character in the regime $d_i > \sqrt{\eta}$.

Key words. magnetohydrodynamics (MHD) – Sun: magnetic fields – plasmas

1. Introduction

Magnetic reconnection has become the accepted mechanism for explaining a variety of energetic phenomena observed in the solar corona, the Earth's magneto-tail and laboratory plasmas (e.g. Priest & Forbes 2000). Traditional models based on the collisional magnetohydrodynamics however, often fail provide a self-consistent description of reconnection. The difficulty stems from the high electrical conductivities of typical astrophysical plasmas (Spitzer 1962). For resistive effects to be important in say, the solar corona, very high current densities must be present, requiring near singularities – current sheets – in the magnetic field (Parker 1994). Such small length scales generally signal the breakdown of collisional conditions in the plasma.

Faced with this difficulty, a potential remedy is to broaden the traditional MHD description by employing a generalized Ohm's law, which includes collisionless quantities such as finite electron inertia and Hall current effects. Recent studies suggest that Hall currents in particular, can significantly influence the merging process, by altering the geometry of the reconnecting fields and changing the speed of the reconnection (e.g. Bhattacharjee et al. 1999; Birn et al. 2001; Dorelli 2003). Unlike classical "resistive" reconnection, which can be developed in terms of planar two dimensional models, Hall current merging is essentially three dimensional since axial field components are naturally induced by planar reconnecting fields. To what extent the emergence of transient axial fields influences the dynamics of the merging process is not yet fully understood. What can be demonstrated is that Hall currents can either speed up or slow down the merging rate, depending on the symmetries of the merging fields (Craig & Watson 2005).

The aim of the present study is to investigate Hall current reconnection in line tied X-point geometries. Early resistive studies of the X-point problem (Craig & McClymont 1991; Hassam 1992; Craig & Watson 1992) showed, in terms of an eigenmode analysis of the planar field, that small amplitude disturbances could be dissipated surprising quickly, at a rate which depends only logarithmically on the dimensionless resistivity $\eta \simeq 10^{-14.5}$. Later work incorporated the presence of axial field components (McClymont & Craig 1996), plasma inertial effects (McClements et al. 2004) and viscous dissipation (Craig et al. 2005) but the Hall current influence was neglected. Our present purpose is to remedy this omission by exploring how Hall currents can affect the Ohmic dissipation rate, the speed of the reconnection, and the morphology of the merging fields.

In Sect. 2 we formulate the X-point reconnection problem in a way which highlights the modifications introduced by the Hall current. In Sect. 3 we present a computational study in which scaling laws are derived for the decay rate and oscillation frequency of arbitrary X-point disturbances. We also study how Hall currents influence the initial implosive collapse that acts as a precursor for the oscillatory decay.

2. MHD with a generalized Ohm's law

We work with the compressible MHD equations, scaled with respect to the reference coronal values (Craig et al. 2003)

$$B_c = 10^2 \text{ G}, \qquad l_c = 10^{9.5} \text{ cm}$$
$$n_c = 10^9 \text{ cm}^{-3}, \quad v_A = 10^9 \text{ cm s}^{-1}.$$

Time is now measured in units of the Alfvén time $\tau_A = l_c/v_A$, which is typically a few seconds in coronal applications. In this formulation the plasma resistivity is an inverse Lundquist number $\eta \ll 1$.

We assume that the behavior of a plasma with density ρ, velocity $\boldsymbol{v}$, pressure p, and magnetic field $\boldsymbol{B}$ is governed by the continuity equation

$$\frac{\partial \rho}{\partial_t} + \nabla \cdot (\rho \boldsymbol{v}) = 0, \tag{1}$$

⋆ This work was supported by the New Zealand Marsden Fund.

Article published by EDP Sciences and available at http://www.edpsciences.org/aa or http://dx.doi.org/10.1051/0004-6361:20054391

the momentum equation,

$$\rho\frac{\partial \boldsymbol{v}}{\partial t} + (\boldsymbol{v}\cdot\nabla)\boldsymbol{v} = -\nabla p + \boldsymbol{J}\times\boldsymbol{B} + \nu\left(\nabla^2\boldsymbol{v} + \frac{1}{3}\nabla(\nabla\cdot\boldsymbol{v})\right), \tag{2}$$

where $\boldsymbol{J} = \nabla\times\boldsymbol{B}$ is the current density, and the generalized induction equation

$$\frac{\partial \boldsymbol{B}}{\partial t} = \nabla\times(\boldsymbol{v}\times\boldsymbol{B}) - \eta\nabla\times\boldsymbol{J} - d_{\rm i}\,\nabla\times(\boldsymbol{J}\times\boldsymbol{B} - \nabla p_{\rm e})$$
$$-d_{\rm e}\nabla\times\left(\frac{\partial \boldsymbol{J}}{\partial t} + (\boldsymbol{v}\cdot\nabla)\boldsymbol{J}\right). \tag{3}$$

Note that the last three terms on the right hand side of Eq. (3) define, respectively, the resistive, Hall and electron inertial term contributions from the generalized Ohm's law. Here

$$\eta = \frac{c^2}{4\pi v_{\rm A} l_{\rm c}\sigma} \simeq 10^{-14.5}$$

is the dimensionless plasma resistivity based on the collisional conductivity,

$$d_{\rm i} = \frac{c}{l_{\rm c}\omega_{\rm pi}} \simeq 10^{-6.5}$$

is the ion skin depth and

$$d_{\rm e} = \left(\frac{c}{l_{\rm c}\omega_{\rm pe}}\right)^2 \simeq 10^{-16}$$

is the electron inertial depth (Spitzer 1962). In the present system the resistivity provides the only avenue for extracting energy from the magnetic field. The Hall term influences the advection of the $\boldsymbol{B}$-field which is now tied mainly to the electron fluid as opposed to the mass-averaged electron-proton gas of conventional MHD. Although, in this paper, we neglect electron inertia and viscous effects by setting $\nu = d_{\rm e} = 0$, these contributions have been explored in recent X-point studies by McClements et al. (2004) and Craig et al. (2005). For the moment we note that the key assumption of Hall current merging is that reconnection length scale $r_{\rm s}$ satisfies $d_{\rm e} \ll r_{\rm s} \le d_{\rm i}$ (Fitzpatrick 2003). Since the collisional merging model we consider predicts $r_{\rm s} \simeq \sqrt{\eta}$ we see that the conditions of Hall MHD are quite likely to be met. Our aim therefore is to study the relative importance of the Hall and resistive terms, and to examine how the geometry of the merging affects both the reconnection and Ohmic dissipation rates.

2.1. Linearized equations

In general the continuity momentum and induction equations need to be supplemented by an equation of state and the conservation law $\nabla\cdot\boldsymbol{B} = 0$. However, since we deal with small displacements in a cold, two and a half dimensional plasma with $\partial_z = 0$, we can obtain a complete description by linearizing Eqs. (2) and (3), and using a flux function representation for the planar magnetic field

$$\boldsymbol{B}(x,y,t) = \nabla\psi\times\hat{\boldsymbol{z}} + Z\hat{\boldsymbol{z}}. \tag{4}$$

In this case the velocity and magnetic fields split naturally into planar and axial components

$$\boldsymbol{v}(x,y,t) = (\boldsymbol{V}, W), \qquad \boldsymbol{B}(x,y,t) = (\partial_y\psi, -\partial_x\psi, Z), \tag{5}$$

where $\boldsymbol{V}\cdot\hat{\boldsymbol{z}} = 0$. It is convenient to let

$$\psi(x,y,t) \to \psi_E(x,y) + \psi(x,y,t), \tag{6}$$

and to linearize about the planar, background field $\boldsymbol{B}_E = (\partial_y\psi_E, -\partial_x\psi_E)$. Small displacements about the equilibrium are now governed by

$$\frac{\partial \boldsymbol{V}}{\partial t} = -\nabla^2\psi\,\nabla\psi_E, \tag{7}$$

$$\frac{\partial W}{\partial t} = (\boldsymbol{B}_E\cdot\nabla)\,Z, \tag{8}$$

$$\frac{\partial \psi}{\partial t} + \boldsymbol{V}\cdot\nabla\psi_E = \eta\nabla^2\psi - d_{\rm i}(\boldsymbol{B}_E\cdot\nabla)\,Z, \tag{9}$$

and

$$\frac{\partial Z}{\partial t} = (\boldsymbol{B}_E\cdot\nabla)W + \eta\nabla^2 Z + d_{\rm i}(\boldsymbol{B}_E\cdot\nabla)\,\nabla^2\psi. \tag{10}$$

This system provides our basic model for describing X-point, Hall current reconnection.

2.2. Preliminary comments

In the absence of the Hall term ($d_{\rm i} = 0$), it is possible to consider a purely planar problem with $Z = W = 0$. In this case the current density, namely

$$\boldsymbol{J} = \left(Z_y, -Z_x, -\nabla^2\psi\right), \tag{11}$$

comprises only an axial "reconnection" current of magnitude $|\nabla^2\psi|$. Merging is now completely defined by the planar Eqs. (7) and (9). For $d_{\rm i}$ finite however, gradients of the reconnection current along the equilibrium field induce a growth in the Z-field (Eq. (10)) which in turn generates an axial velocity W (Eq. (8)). Growth in the axial components can be expected to feed back on the flow field and slow down the merging process. In general both the reconnection rate, namely

$$\frac{\partial \psi}{\partial t} = \eta|\boldsymbol{J}_0| \tag{12}$$

where $\boldsymbol{J}_0$ is the current density at the merging point, and the Ohmic dissipation rate

$$W_\eta = \eta\int J^2{\rm d}V = \eta\int\left(Z_x^2 + Z_y^2 + \left(\nabla^2\psi\right)^2\right){\rm d}V, \tag{13}$$

will be affected by the growth in Z.

We can estimate the conditions under which the Hall term becomes important by comparing $\eta\nabla^2\psi$ with $d_{\rm i}(\boldsymbol{B}_E\cdot\nabla)Z$ in Eq. (9). Assuming the Z-field is induced from Eq. (10), we see that we require

$$\kappa = \tau_{\rm M}\frac{{d_{\rm i}}^2}{\eta} \ge 1 \tag{14}$$

where $\tau_{\rm M}$ is a typical merging timescale. Even for Alfvénic merging where $\tau_{\rm M} = O(1)$, this condition is easily met for the reference values $\eta \simeq 10^{-14.5}, d_{\rm i} \simeq 10^{-6.5}$. Hence, we have good grounds for including Hall currents in reconnection models based on collisional conductivities.

3. X-type neutral points with Hall currents

3.1. Initial conditions

Although the resistive problem ($d_i = 0$) can be described analytically using a cylindrical mode decomposition, the directional derivatives associated with the Hall term $\boldsymbol{B}_E \cdot \nabla$ preclude a similar analytic study. Accordingly, we adopt an entirely computational approach when we study the influence of the Hall current. In this respect our study is similar to Fitzpatrick (2003) who considered the role of Hall currents in the Taylor problem based on the one-dimensional background field $\psi_E = -x^2/2$.

In what follows we consider an equilibrium X-point

$$\psi_E = xy \qquad -1 \le x, y \le 1 \tag{15}$$

located at the centre of a highly conducting square boundary. The field is immersed in a uniform density plasma and anchored by line-tying to rigid outer walls where $\boldsymbol{v} = 0$ and the potential ψ is fixed. We assume initial conditions in which

$$V(x, y, 0) = Z(x, y, 0) = W(x, y, 0) = 0, \tag{16}$$

so that only the planar field ψ is disturbed. The effect of the disturbance is to raise the energy of the X-point and change its intrinsic topology.

A typical initial condition is shown in Fig. 1a, based on the reconnection disturbance field

$$\psi(x, y, 0) = A\left(1 - x^2\right)\left(1 - y^2\right) \tag{17}$$

with $A = 0.1$. This form of disturbance alters the flux in each lobe of the X-point and sets up a Lorentz force which accelerates the plasma inwards. A similar X-point topology could be set up by the approach of two sub-photospheric dipoles. Either way, the collapse is halted only when the excess flux in the two broad lobes is transferred by reconnection through the neutral point. In fact the plasma tends to overshoot on the initial implosion, transferring too much flux to the narrower lobes. It is this "inertial overshoot" that sets up the conditions required for oscillatory reconnection.

It should be mentioned that the validity of the linearized solution is dependent on the level of the plasma resistivity (in fact $A \le \eta$). If the perturbation amplitude is too large the linearization breaks down – the current density loses its cylindrical structure and becomes quasi one-dimensional in the vicinity of the origin. Finite amplitude effects have been considered by McClymont & Craig (1996), but here we will assume that parameters are chosen so that the linear reconnection solution remains valid.

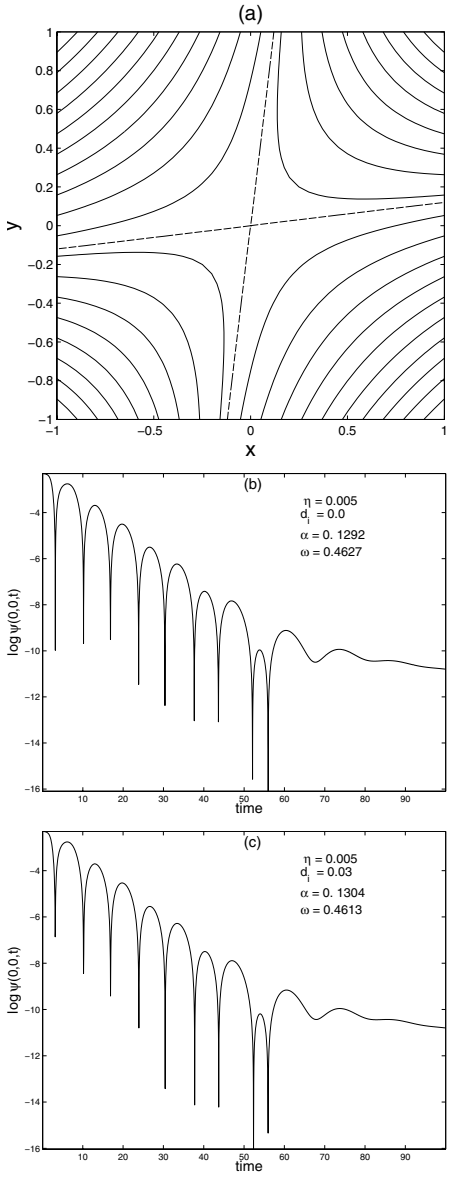

Fig. 1. a) Field lines of the perturbed X-point configuration with potential field $\psi = xy + 0.1(1 - x^2)(1 - y^2)$. **b**) Plot showing decay of the flux function ψ versus time (measured in Alfvén times) when $d_i = 0$, $\eta = 0.005$. **c**) Plot showing decay of ψ at the neutral point when $d_i = .03$ with $\eta = 0.005$. After a certain number of Alfvén times, both ψ functions ceases to oscillate.

3.2. Resistive X-point decay

In the case $d_i = 0$ the reconnection problem can be reduced to the analytic X-point solution of Craig & McClymont (1991, 1993) and Hassam (1992). As summarized in Fig. 1b, the resistive solution comprises three distinct phases: there is an initial implosion in which the disturbance localizes into a quasi-cylindrical current spike of amplitude $J \sim \eta^{-1}$ at the origin. This is followed by a phase of oscillatory reconnection, dominated by the fundamental eigenmode,

$$\lambda = \alpha + \mathrm{i}\omega, \quad \alpha = -\frac{\omega^2}{2}, \quad \omega = \frac{\pi}{|\ln \eta|}. \tag{18}$$

Finally, after the oscillations have died down, and the bulk of the disturbance energy has been removed, a self-similar mode emerges associated with a very slow monotonic decay. Note that the initial implosion is very rapid – it takes only a few Alfvén times for the oscillatory modes to set in.

A key result of the resistive computation is that the main oscillatory phase of the energy decay depends at most logarithmically on the plasma resistivity η. It follows that the resistive solution provides an analytic model of fast reconnection. More physically, the fundamental oscillation frequency ω can be understood as the "bounce-time" for an Alfvén wave, launched from the outer wall – idealized for analytic purposes as a cylinder of unit radius – to return from traversing the diffusion region ($r < r_s \simeq \sqrt{\eta}$). That is,

$$\frac{1}{\omega} \simeq \frac{2}{\pi} \int_{r_s}^{1} \frac{\mathrm{d}r}{v_A} \simeq \frac{2}{\pi} |\ln(r_s)|, \tag{19}$$

since $v_A = r$ is defined by the background field $\boldsymbol{B}_E$. Independent computations (Craig & Watson 1992; Craig et al. 2005) confirm

that the eigenmodes description remains an excellent approximation when the circular boundary is replaced by a highly conducting square wall.

3.3. Numerical solutions with Hall effects

We focus on three aspects of the reconnection solutions, namely how Hall currents influence:

- the frequency and decay rate of oscillatory X-point modes;
- the resistive scalings associated with the initial implosion of the disturbances field;
- the morphology of the localized current region at the center of the X-point.

Numerical solutions are obtained in two ways: either by an explicit finite difference replacement of system (7) to (10); or by eliminating the velocity fields and using a semi-implicit treatment of

$$\psi_{tt} = r^2\nabla^2\psi + \eta\nabla^2\psi_t - d_{\rm i}\mathcal{D}Z_t \tag{20}$$

$$Z_{tt} = \eta\nabla^2 Z_t + \mathcal{D}(\mathcal{D}Z + d_{\rm i}\nabla^2\psi_t), \tag{21}$$

where

$$\mathcal{D} = \boldsymbol{B}_E\cdot\nabla = x\partial_x - y\partial_y$$

defines the directional derivative along the equilibrium field. The results which follow have been checked for consistency using both numerical techniques.

3.4. Decay rate and oscillation frequency

Our first observation, based on Figure 1c, is that the decay of the disturbance field (17) when $d_{\rm i} \neq 0$, maintains the three distinct phases of Fig. 1b. We begin therefore by examining the decay rate α and oscillation frequency ω for various values of $d_{\rm i}$, taking a fixed value of the resistivity η. Suppose α_0 and ω_0 denote rates in the case $d_{\rm i} = 0$. Then the results of Fig. 2a, based on $\eta = 0.01$, suggest that there is a linear relation between $\ln(\alpha - \alpha_0)$ and $\ln(d_{\rm i}\eta^{-1/4})$. Since computations at other η values (Fig. 2b) reinforce this relationship we obtain a scaling law for the decay rate

$$\alpha = \alpha_0 + a_1\left(\frac{d_{\rm i}}{\eta^{1/4}}\right)^{r_1}, \tag{22}$$

with $a_1 \simeq 0.1$ and $r_1 \simeq 2$. This relationship holds for $0 \le \kappa = d_{\rm i}^2/\eta \simeq 2$, and confirms that increases in the Hall coefficient enhance the decay rate of the plasma.

A similar relationship holds for ω. But, as summarized in Figs. 3a and b, the oscillation frequency is found to *decrease* with increases in $d_{\rm i}$:

$$\omega = \omega_0 - a_1\left(\frac{d_{\rm i}}{\eta^{1/4}}\right)^{r_1}. \tag{23}$$

These scalings confirm that Hall current reconnection breaks the simple analytic relationship between the oscillation frequency and the decay rate found in the resistive problem (18). One possible explanation – and one that holds for the related problem of steady state incompressible merging (Dorelli 2003; Craig & Watson 2005) – is that the Hall current speeds up the merging rate by enhancing the localization of the current density. This would indeed slow down the oscillation frequency since, by the argument leading to Eq. (19), $r_{\rm s}$ is taken to be smaller than its resistive value. The veracity of this argument depends however, on the detailed morphology of the current density, and this can change dramatically when the Hall term is sufficiently large, as we detail below. A further difficulty is that stronger current densities for $d_{\rm i} > 0$ will increase the tendency for current driven instabilities, especially when it is remembered that ion-acoustic turbulence is likely to be excited for purely collisional merging (Litvinenko & Craig 2000).

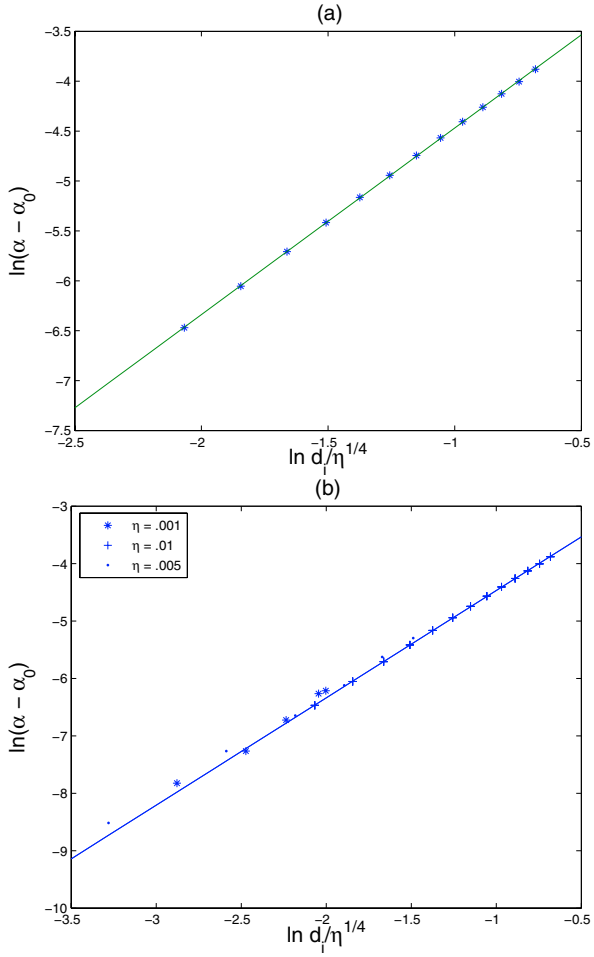

Fig. 2. Scaling of the decay rate, α, as the function of $d_{\rm i}$ in oscillatory phase for the parameters **a**) $\eta = 0.01$ with range $0.01 \le \kappa \le 2.56$ and **b**) $\eta = 0.01$, 0.005 and 0.001 with range $0.01 \le \kappa \le 2.56$ where $\kappa = d_{\rm i}^2/\eta$. The solid lines in both plots are fit to $\ln(\alpha - \alpha_0) \simeq 2\ln(d_{\rm i}/\eta^{1/4}) + \ln(0.1)$.

3.5. The initial X-point implosion

We have already mentioned that both the reconnection rate (12) and the Ohmic dissipation rate (13) are largely independent of resistivity in the purely collisional solution. Specifically, the cylindrical solution implies that, during the initial implosive phase, the current density localizes over a small circular area A according to

$$J_0 \sim \frac{1}{\eta}, \quad A \sim {r_{\rm s}}^2 \sim \eta, \tag{24}$$

where $\boldsymbol{J} = -\nabla^2\psi\,\hat{\boldsymbol{z}}$. These relations suggest that both the reconnection rate ηJ_0 and the Ohmic dissipation rate $W_\eta \simeq \eta J_0^2 A$ should scale independent of resistivity.

In Fig. 4 we show computations of W_η and $\psi_t = \eta J_0$ during the first ten Alfvén times. It is clear that, although the time to

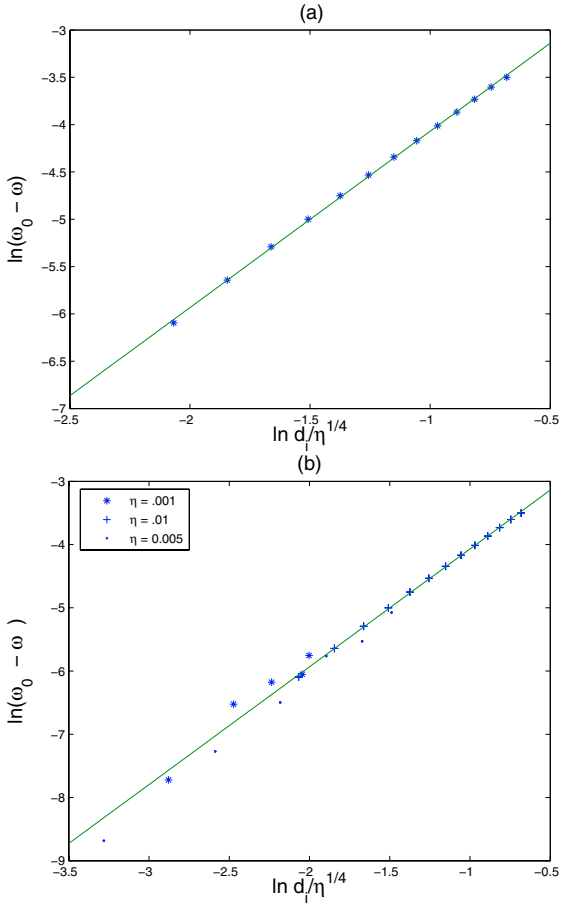

Fig. 3. Scaling of the oscillation frequency, ω, as the function of d_i in the oscillatory phase for the parameters **a**) $\eta = 0.01$ with range $0.01 \leq \kappa \leq 2.56$ and **b**) $\eta = 0.01$, 0.005 and 0.001 with range $0.01 \leq \kappa \leq 2.56$ where $\kappa = d_i^2/\eta$. The solid lines in both plots are fits to $\ln(\omega_0 - \omega) \simeq 2\ln(d_i/\eta^{1/4}) + \ln(0.1)$.

achieve the maximum dissipation rate increases with reductions in η, the peak rates remain, in agreement with theory, unaffected by decreases in resistivity.

The inclusion of Hall currents means that the current density is no longer purely axial – planar components are present due to the induction of the Z-field. Such components cannot directly influence the reconnection rate since flux transfer at the neutral point depends only on the axial current $\nabla^2\psi\,\hat{\boldsymbol{z}}$. However, by increasing the overall amplitude of the current density, they could directly enhance the global Ohmic dissipation rate.

Figures 5a and b show the variation of reconnection rate ηJ_0 with the magnitude of the Hall term when $\eta = 0.01$ and 0.003 respectively. At first, the peak reconnection rate slightly decreases with increasing d_i, achieving a minimum reconnection rate at $d_i = d_i^*$ say. Fitzpatrick (2003) observed broadly similar behaviour for the Taylor problem, but in his case the reconnection rate was independent of d_i, for $d_i < d_i^*$ with d_i^* scaling as $d_i^* \sim \eta^{1/3}$. In Fig. 6a we plot the logarithm of the reconnection rate against $\log(d_i)$, for three values of η and note the systematic shift to the right of the minimum rate. However, since Fig. 6b indicates that this shift can be eliminated if the reconnection rate is plotted against $\log(d_i/\eta^{1/3})$ we obtain the tentative result that d_i^* may scale as $\eta^{1/3}$. The reconnection rate increases for $d_i > d_i^*$ where there is an increasing tendency for the reconnection rate to oscillate (Fig. 5). The development of oscillatory components in Hall current solutions has been noted in previous studies (e.g.

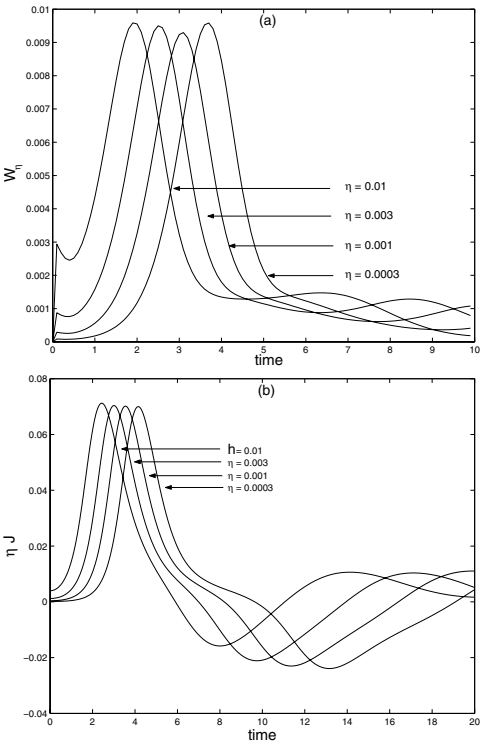

Fig. 4. a) The Ohmic dissipation rate, W_η, versus time. **b**) The reconnection rate, ηJ, versus time for various values of resistivity. The maximum (peak) rates are largely unaffected by resistivity in both cases.

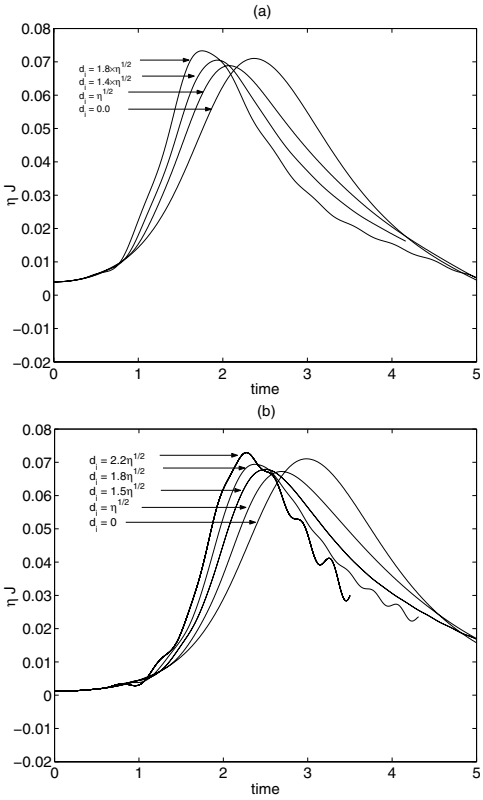

Fig. 5. The reconnection rate, ηJ, versus time for various values of d_i when **a**) $\eta = 0.01$ and **b**) $\eta = 0.003$.

Watson & Porchelli 2004) and may be linked to the development of whistler wave modes in the solution for large $d_i \gg \sqrt{\eta}$ (see Sect. 3.6 below).

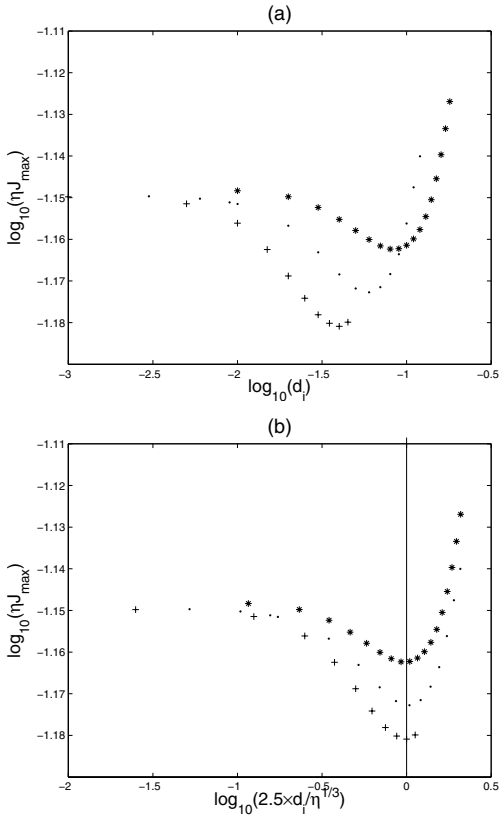

Fig. 6. a) Scaling of the peak magnetic reconnection rate, ηJ, with the collisionless ion skin depth, d_i, in the linear regime. **b**) Scaling of the peak magnetic reconnection rate, ηJ, with $2.5 \times d_\mathrm{i}/\eta^{1/3}$. The "*" corresponds to $\eta = 0.01$. The "." corresponds to $\eta = 0.003$. The "+" corresponds to $\eta = 0.001$.

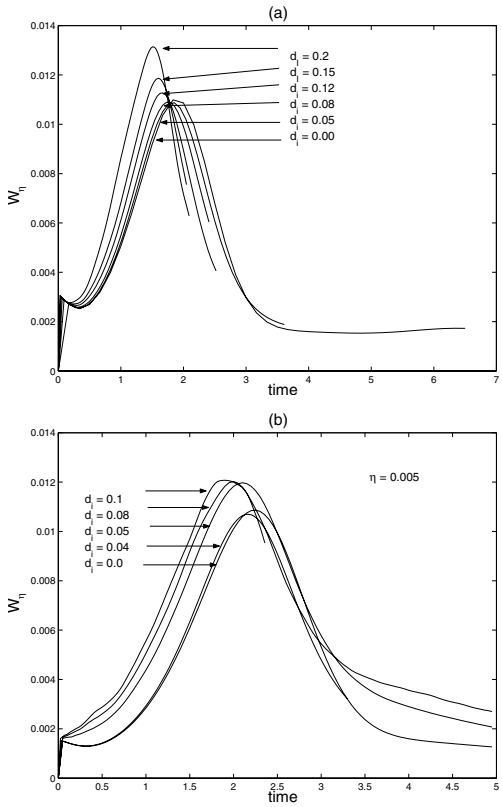

Fig. 7. The Ohmic dissipation rate versus time for various values of the collisionless ion skin depth, d_i, for **a**) $\eta = 0.01$, **b**) $\eta = 0.005$.

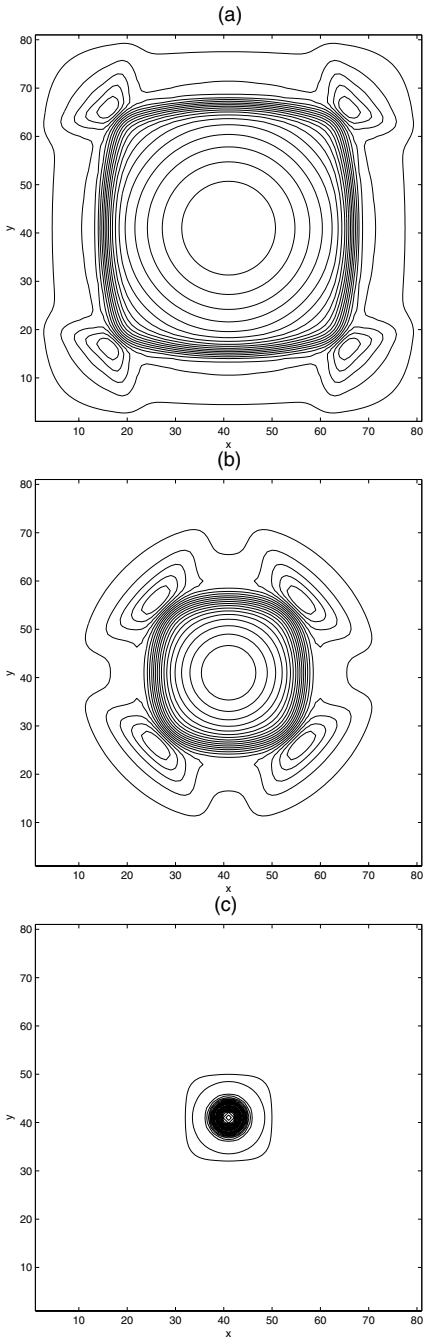

Fig. 8. Localization of current density($-\nabla^2\psi\,\hat{\mathbf{z}}$) contours for $d_\mathrm{i} = 0$, and $\eta = 0.005$, after **a**) 1/2 Alfvén time, **b**) 1 Alfvén time and **c**) time of maximum current ($t \sim 2$).

The Ohmic dissipation rate is less ambiguous. Although the Ohmic rate is largely unaffected for small values of the Hall term, the evidence suggests that the Hall-induced axial field, can lead to enhanced dissipation over traditional models with $d_\mathrm{i} = 0$. This enhancement can partly be attributed to the induced planar currents for finite d_i, but we should also bear in mind, as discussed below, that the changing solution geometry could also be influential.

3.6. Structure of the imploding field

In Fig. 8 we show the purely resistive localization of the axial current at three different Alfvén times ($\eta = 0.005, d_\mathrm{i} = 0$). The plots highlight the initial implosive phase as the

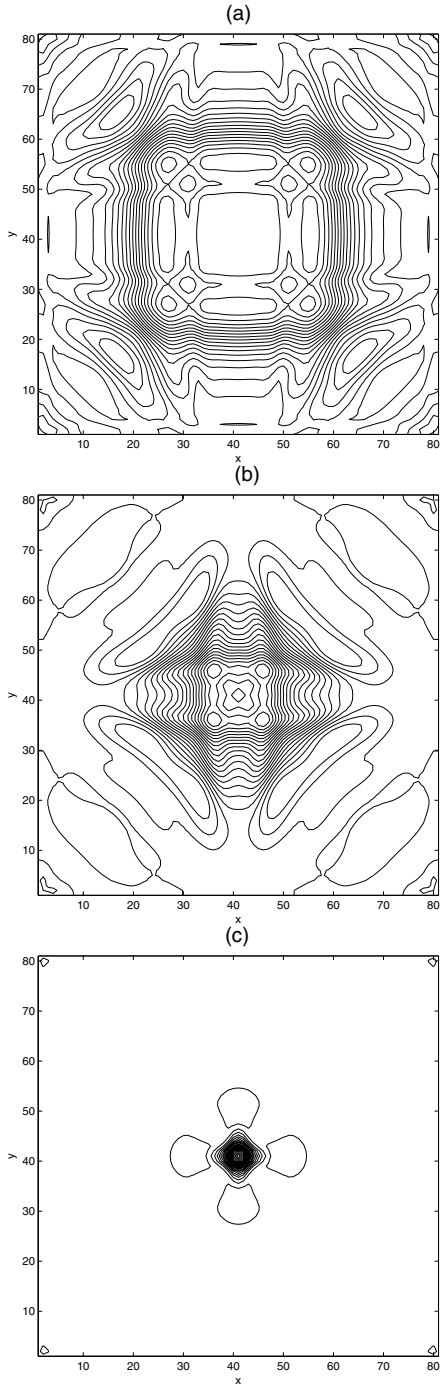

Fig. 9. Localization of current density($-\nabla^2\psi\,\hat{z}$) contours for $d_\mathrm{i} = \sqrt{\eta}$, and $\eta = 0.005$, after **a**) 1/2 Alfvén time, **b**) 1 Alfvén time and **c**) time of maximum current ($t \sim 2$).

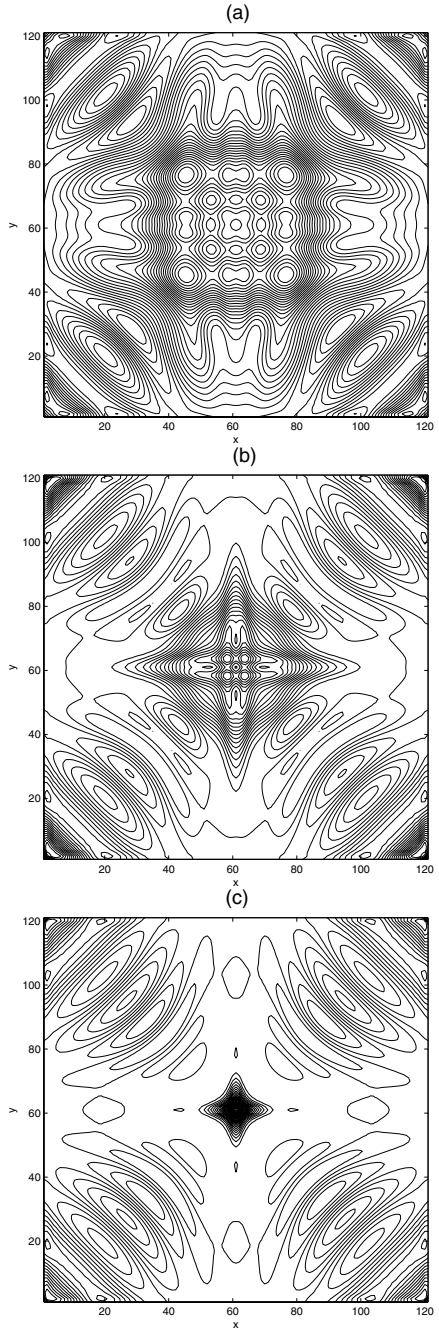

Fig. 10. Localization of current density($-\nabla^2\psi\,\hat{z}$) contours for $d_\mathrm{i} = 2\sqrt{\eta}$, and $\eta = 0.005$, after **a**) 1/2 Alfvén time, **b**) 1 Alfvén time and **c**) time of maximum current ($t \sim 2$).

disturbance field propagates towards the neutral point. As mentioned in Sect. 3.5, the reconnecting current winds up localized in a quasi-cylindrical spike of area η and amplitude η^{-1} centered on the origin. In particular the current contours close to the diffusion region remain approximately circular for all times up to the time of current maximum ($t \simeq 2$).

In Figs. 9 and 10 we perform identical computations but include the influence of the Hall current, $d_\mathrm{i} = \sqrt{\eta}$ and $d_\mathrm{i} = 2\sqrt{\eta}$ respectively. It is clear that morphology of the current changes markedly when the Hall term is added. For $d_\mathrm{i} \simeq \sqrt{\eta}$ the current contours (Fig. 9) develop a quadripolar tendency but localization is still achieved by the time of current maximum. Figure 10 shows however, that for runs with a sufficiently large Hall parameter $d_\mathrm{i} = 2\sqrt{\eta}$, current localization may be significantly compromized. A central spike is still present but the outer field now shows a series of current corrugations aligned to the background field. It is interesting that similar stratifications (for $d_\mathrm{i} \gg \sqrt{\eta}$) have been observed for incompressible, steady state merging in open X-point geometries (Craig & Watson 2003). The most likely explanation is the emergence of whistler wave modes for sufficiently large d_i. Such modes are not effectively controlled by collisional resistivities and a heuristic "hyper resistivity " is often invoked in computational studies to damp down the high frequency development (Fitzpatrick 2003). More fundamentally,

the need for such expedients probably indicates the physical incompleteness of the generalized MHD system under study.

4. Conclusions

We have considered dynamic Hall-current reconnection in line-tied, magnetic X-points. The X-point evolution is formulated as an initial value problem governed by two small external parameters, the dimensionless resistivity η and the normalized ion skin depth d_i. Physical considerations suggest that the Hall current can significantly alter the resistive solution ($d_\mathrm{i} = 0$) when

$$d_\mathrm{i} \simeq \eta^{1/2},$$

a condition which is easily satisfied for collisional coronal plasmas ($\eta \simeq 10^{-14.5}$, $d_\mathrm{i} \simeq 10^{-6.5}$). One consequence of X-point reconnection in the presence of the Hall term is the development of axial field components which feed back on the system and alter the reconnection rate. In the present computation such components remain zero for all time when the Hall current is switched off.

The present computations show that the Hall current can manifest itself in several distinct ways. For purely resistive plasmas ($d_\mathrm{i} = 0$), the main dissipation phase is dominated by oscillatory eigenmodes whose frequency and decay rate depend only logarithmically on the plasma resistivity. These Alfvénic modes persist for $d_\mathrm{i} > 0$, and although the oscillation rate is reduced, the decay rate is notably enhanced. Scaling laws summarizing this behaviour are presented in Sect. 3.4 and these suggest stronger localizations of the current density for $d_\mathrm{i} > 0$.

We have also emphasized that Hall currents influence the transient implosion phases which act as a precursor to the eigenmode development. Although the Ohmic dissipation rate resulting from initial collapse is enhanced, the reconnection rate behaves more ambiguously in that it suffers an initial decline before increasing for $d_\mathrm{i} > d_\mathrm{i}^*$ as shown in Fig. 6. The structure of the reconnection current also undergoes dramatic changes in this regime: the localized cylindrical currents which dominate the purely resistive calculation, eventually give way to current corrugations, aligned to the background field, which extend throughout the X-point. This behaviour has also been witnessed in computations of incompressible merging in open geometries, and may provide a useful signature for identifying strong Hall current effects (Craig et al. 2003). Such current corrugations are probably a signature of whistler wave modes whose high frequencies are not effectively damped by purely collisional resistivities.

In summary, the present X-point computations confirm that Hall currents can influence reconnection rates, Ohmic dissipation rates and the geometry of the reconnecting fields in a variety of ways. Although we have considered only small amplitude disturbances about a planar X-point, it clear that many of our findings are consistent with Hall current merging studies in other geometries (Dorelli 2003; Fitzpatrick 2003). In particular, when reconnection rates are enhanced by Hall effects, the current localization becomes more intense and the problem of exceeding current density thresholds based on the ion-acoustic limit – already a problem in conventional MHD – may be worsened. It follows that the inclusion of a generalized Ohm's law, may still be insufficient to provide a realistic description of magnetic merging based on collisional resistivities.

References

Bhattacharjee, A., Ma, Z. W., & Wang, X. 1999, JGR, 104, 14543
Birn, J., & Hesse, M. 2001, JGR, 106, 3737
Craig, I. J. D., Heerikhuisen, J., & Watson, P. G. 2003, PhPl, 10, 3120
Craig, I. J. D., & McClymont, A. N. 1991, ApJ, 371, L41
Craig, I. J. D., & McClymont, A. N. 1993, ApJ, 405, 207
Craig, I. J. D., & Watson, P. G. 1992, ApJ, 393, 385
Craig, I. J. D., & Watson, P. G. 2005, PhPl, 12a, 2306
Craig, I. J. D., Litvinenko, Y. E., & Senanayake, T. 2005, A&A, 433, 1139
Dorelli, J.C. 2003, PhPl, 10, 3309
Fitzpatrick, & Richard 2004, PhPl, 11, 937
Hassam, A. B. 1992, ApJ, 339, 159
Litvinenko, Y. E., & Craig, I. J. D. 2000, ApJ, 544, 1101
McClements, K. G., Thyagaraja, A., Ben Ayed, N., & Fletcher, L. 2004, ApJ, 609, 423
McClymont, A. N., & Craig, I. J. D. 1996, ApJ, 466, 487
Parker, E. N. 1994, Spontaneous current sheets in magnetic fields (Oxford University Press)
Priest, E., & Forbes, T. 2000, Magnetic Reconnection (Cambridge University Press)
Spitzer, L. 1962, Physics of fully ionized gases (John Wiley & Sons)
Watson, P. G., & Porcelli, F. 2004, ApJ, 617, 1353